CHEMISTRY OF MATERIALS
Article

Chem. Mater. **2010,** *22,* 4749–4755 4749
DOI:10.1021/cm101193g

2-Aminopyrimidine-Silver(I) Based Hybrid Organic Polymers: Self-Assembly and Phase Transitions of a Novel Class of Electronic Material

Ion Stoll,*[,†] Regina Brockhinke,[†] Andreas Brockhinke,[†] Markus Böttcher,[†] Thomas Koop,[†] Hans-Georg Stammler,[†] Beate Neumann,[†] Andrea Niemeyer,[‡] Andreas Hütten,[‡] and Jochen Mattay*[,†]

[†]*Organic Chemistry I, Department of Chemistry and* [‡]*Department of Physics, Thin Films & Physics of Nanostructures, Bielefeld University, Universitätsstrasse 25, 33615 Bielefeld, Germany*

Received April 28, 2010. Revised Manuscript Received June 25, 2010

Solution processing methods of conjugated polymers are an important strategy for the preparation of organic semiconductors. We introduce a novel family of semiconductors prepared by the solution based small molecule self-assembly of 2-amino-5-pentafluorophenylpyrimidine and various silver(I) salts (AgX; X = CO_2CF_3, SO_3CF_3, NO_3). The compounds are analyzed by single crystal analysis revealing that the solid state assembly consists of alternating polymer strands of 2-aminopyrimidine and silver(I). The solid state assembly can be controlled by the silver counterion and the solvent yielding polymer strands with different interatomic parameters and optoelectrical properties. The compounds are optically characterized and reveal remarkably different solid state absorption when compared to the parent compound 2-aminopyrimidine in solution. Also, an exclusive solid state emissive state is observed. Herein, the excitation occurs not at the maximum but at the onset of absorbance. The silver(I)triflate-2-aminopyrimidine yields two different porous frameworks depending on the solvent used for crystallization. These porous frameworks are made of 1-dimensional polymer strands, and the pores are filled with solvent molecules. By heating and addition of solvent the frameworks can be reversibly converted into each other in the solid state, changing the optoelectrical properties. The compounds are thermodynamically analyzed by differential scanning calorimetry. Also, the electrical conductance was proven in a preliminary experiment on a thin crystalline film of **4**.

Introduction

Organic semi- and photoconductors are important materials for various applications because of their low cost fabrication processes and the possibility to fine-tune desired functions by chemical modification of their building blocks. Conductive organic materials with different features are known, and formidable progress has been made in the field of hybrid light emitting diodes with organic emitters and organic field-effect transistors.[1−6] A more recent area of research is to apply organic semiconductors in spintronic devices.[7] Apart from the chemical properties of the building blocks of an (opto)electronic device the electrical and optical characteristics are largely emerging from the solid state assembly of the organic building blocks. For this assembly, solution processing and gas phase deposition are the established processing techniques, and they can be controlled by experimental parameters (concentration, pressure, temperature), which are often limited to the nature of the compounds used.[8] Controlling the supramolecular organization of the electronic material is an important approach to manage problems because of the degree of ordering in the solid state.[9] On a supramolecular level one can distinguish between the molecular and crystalline assembly (leading to material defects and impurity doping) on the one hand and the morphology of the formed solid state assembly on the other hand. The key properties of conductive materials like charge transport mobility and carrier type, transport anisotropy, transfer integral, the band gap, and so forth are directly associated with the supramolecular assembly,[10,11] emphasizing the importance of a controlled supramolecular

*To whom correspondence should be addressed. E-mail: oc1jm@uni-bielefeld.de (J.M.), ion_philipp.stoll@uni-bielefeld.de (I.S.).

(1) Saito, G.; Yoshida, Y. *Bull. Chem. Soc. Jpn.* **2007**, *80*, 1–137.
(2) Kraft, A.; Grimsdale, A. C.; Holmes, A. B. *Angew. Chem.* **1998**, *110*, 416–443. Kraft, A.; Grimsdale, A. C.; Holmes, A. B. *Angew. Chem., Int. Ed.* **1998**, *37*, 402–428.
(3) Friend, R. H.; Gymer, R. W.; Holmes, A. B.; Burroughes, J. H.; Marks, R. N.; Taliani, C.; Bradley, D. D. C.; Dos Santos, D. A.; Brédas, J. L.; Lögdlund, M.; Salaneck, W. R. *Nature* **1999**, *397*, 121–128.
(4) Kelley, T. W.; Baude, P. F.; Gerlach, C.; Ender, D. E.; Muyres, D.; Haase, M. A.; Vogel, D. E.; Theiss, S. D. *Chem. Mater.* **2004**, *16*, 4413–4422.
(5) Facchetti, A.; Yoon, M.-H.; Marks, T. J. *Adv. Mater.* **2005**, *17*, 1705–1725.
(6) Wallikewitz, B. H.; Hertel, D.; Meerholz, K. *Chem. Mater.* **2009**, *21*, 2912–2919.
(7) Dediu, V. A.; Hueso, L. E.; Bergenti, I.; Taliani, C. *Nat. Mater.* **2009**, *8*, 707–716.
(8) Allard, S.; Forster, M.; Souharce, B.; Thiem, H.; Scherf, U. *Angew. Chem.* **2008**, *120*, 4138–4167. Allard, S.; Forster, M.; Souharce, B.; Thiem, H.; Scherf, U. *Angew. Chem., Int. Ed.* **2008**, *47*, 4070–4098.
(9) Schmaltz, B.; Weil, T.; Müllen, K. *Adv. Mater.* **2009**, *21*, 1067–1078.
(10) Brédas, J. L.; Calbert, J. P.; da Silva Filho, D. A.; Cornil, J. *Proc. Natl. Acad. Sci. U.S.A.* **2002**, *99*, 5804–5809.
(11) Fichou, D. *J. Mater. Chem.* **2000**, *10*, 571–588.

Published on Web 07/20/2010

assembly of electronic materials. 2-Aminopyrimidines are a class of compounds which are suitable for solid state self-assembly by non-covalent interactions,[12,13] and closely related nitrogen-based heterocyclic molecules and silver(I) based complexes have recently been employed in the design of organic semiconductors.[14−16] Various silver(I) complexes of 2-aminopyrimidines are known, and silver coordination is a versatile tool for the self-assembly of 2-aminopyrimidines in the solid state. Several silver-based coordination polymers have been described in the literature,[17] especially a summary of the various binding modes of silver(I) and 2-aminopyrimdines has been reported in reference 17c. For all these silver complexes the solid state assembly is strongly affected by the silver counterion used. Therefore, the counterion controlled self-assembly is a promising method for the solution based synthesis of organic electronics. Herein, we report the synthesis and characterization of new metal organic coordination polymers suitable for electronic materials based on perfluorinated arene functionalized 2-aminopyrimidine **2** and silver(I) salts. The semiconducting properties of the compounds are investigated by optical methods showing that these polymers display a new class of conductive materials with an emissive excited state. The optical properties can be easily tuned by changing the silver counterion or by the reversible solvent extrusion and interchange. Also, the electrical conductivity was proven in a preliminary experiment on a thin crystalline film of **4**.

Experimental Section

Materials and Methods. Pentafluorophenyl acetic acid was commercially purchased from Acros Organics. NMR spectra were recorded on a Bruker AM Avance DRX500 spectrometer without external standard. High-resolution mass spectrometry (HRMS) was obtained using 7.0 T Fourier Transform Ion Cyclotron Resonance Mass Spectrometer APEX III, Bruker Daltonik. IR spectra were recorded on a Thermo Electron Nicolet 380 FT IR spectrometer. Elemental analyses were performed on a LECO CHNS-932. Thermodynamic data were determined in DSC measurements using a DSC-Q100 (TA Instruments). Typically measurements were performed in the temperature range from 0 to 300 °C under nitrogen with cooling and heating rates of 10 °C min^{-1}. Absorption is measured with a UV/vis double beam spectrometer (Shimadzu UV-2550). Excitation−emission spectra were obtained by using a custom-built setup with a 75 W Xe lamp, two astigmatism-corrected spectrometers for signal processing, and a back-thinned CCD camera (Roper Scientific) for detection. Details of this method can be found elsewhere.[18] A short-pulse laser system based on a regeneratively amplified Ti:sapphire laser (pulse duration: 3 ps) with subsequent frequency-tripling and detection with a streak camera has been used for simultaneous time- and wavelength-resolved measurements.[19] Electrical conductivity was measured in a two point probe array on a Keithley 2000 Multimeter. Single-crystal X-ray analyses were carried out with a Nonius Kappa-CCD diffractometer by using Mo Kα radiation of the wavelength 0.71073 Å. The structures were solved and refined with SHELX-97[20] with refinements on F^2. All hydrogen atoms were refined isotropically. All hydrogen atoms were refined at calculated positions using a riding model. Basic crystal parameters and structure refinements are summarized in Table S1 (Supporting Information). X-ray powder diffraction measurements were performed on a Philips X'pert pro MPD PW 3040/60 diffractometer using Cu Kα radiation on a glass substrate. X-ray powder diffraction measurements of **2** were performed on a Philips PW 1050/37 diffractometer using Cu Kα radiation on an aluminum substrate.

Synthesis. *l-(Dimethylamino)-3-(dimethyliminio)-2-pentafluorophenyl-prop-l-ene perchlorate* ***1***. 2,3,4,5,6-Pentafluorophenylacetic acid (1 g, 4.4 mmol) was suspended in a mixture of dimethylformamide (3 mL, 2.83 g, 39 mmol) and phosphoryl chloride (2 mL, 3.29 g, 21 mmol) and heated to 80 °C for 3 h. The mixture was given on ice (5 g) and conc. $Mg(ClO_4)_2$ soln (10 mL) was added. The resulting precipitate was filtered off and washed with diluted $Mg(ClO_4)_2$ soln. After recrystallization from ethanol the product was obtained as yellowish solid (1.36 g, 3.4 mmol, 77%). M.p.: 173−177 °C. ^{1}H NMR (500 MHz, $CDCl_3$): δ = 8.18 (s, 2H), 3.43 (s, 6H), 2.69 (s, 6H) ppm. ^{19}F NMR (470 MHz, $CDCl_3$): δ = −135.8 (d, ^3J(F,F) = 17.2 Hz, 2F), −148.9 (s), −159.0 (t, J(F,F) = 17.8 Hz, 2F) ppm. ^{13}C NMR (125 MHz, $CDCl_3$): δ = 165.2, 145.2 (m), 142.3 (m), 137.8 (m), 107.4 (m), 86.6, 49.6, 38.6 ppm. IR (ATR): $\tilde{\nu}$ = 1600, 1525, 1497, 1399, 1081(ClO_4^-), 982, 961, 872, 819, 622 cm^{-1}. HRMS (ESI): m/z calcd for $C_{13}H_{14}F_5N_2$ $[M]^+$: 293.10717; found 293.10685.

5-Pentafluorophenyl-pyrimidin-2-ylamine ***2***. To a suspension of the iminium perchlorate **1** (700 mg, 1.8 mmol) and guanidine hydrochloride (0.4 g, 4 mmol) in *tert*-butanol (40 mL) sodium *tert*-butoxide (0.4 g, 4 mmol) was added and refluxed for 2 h. The solvent was removed in vacuo, and water was added. After filtration the remaining precipitate was recrystallized from ethanol to afford 2 (384 mg, 1.5 mmol, 83%) as colorless solid. ^{1}H NMR (500 MHz, $(CD_3)_2SO$): δ = 8.38 (s, 2H, ArH), 7.17 (2H, s, NH_2) ppm. ^{19}F NMR (470 MHz, $(CD_3)_2SO$): δ = −143.5 (dd, J(F,F) = 24.0 Hz, J(F,F) = 6.9 Hz 2F), −156.5

(12) Stoll, I.; Brodbeck, R.; Neumann, B.; Stammler, H.-G.; Mattay, J. *CrystEngComm* **2009**, *11*, 306–317.
(13) (a) Etter, M. C.; Adsmond, D. A. *J. Chem. Soc., Chem. Commun.* **1990**, 589–591. (b) Krische, M. J.; Lehn, J.-M.; Kyritsakas, N.; Fischer, J.; Wegelius, E. K.; Nissinen, M. J.; Rissanen, K. *Helv. Chim. Acta* **1998**, *81*, 1921–1930. (c) Krische, M. J.; Lehn, J.-M.; Kyritsakas, N.; Fischer, J.; Wegelius, E. K.; Rissanen, K. *Tetrahedron* **2000**, *56*, 6701–6706.
(14) Ortiz, R. P.; Casado, J.; Hernández, V.; López Navarrete, J. T.; Letizia, J. A.; Ratner, M. A.; Facchetti, A.; Marks, T. J. *Chem.—Eur. J.* **2009**, *15*, 5023–5039.
(15) Southward, R. E.; Thompson, D. W. *Chem. Mater.* **2004**, *16*, 1277–1284.
(16) (a) Li, X.-G.; Hua, Y.-M.; Huang, M.-R. *Chem.—Eur. J.* **2005**, *11*, 4247–4256. (b) Li, X.-G.; Huang, M.-R.; Hua, Y.-M. *Macromolecules* **2005**, *38*, 4211–4219. (c) Li, X.-G.; Huang, M.-R.; Jin, Y.; Yang, Y.-L. *Polymer* **2001**, *42*, 3427–3435.
(17) (a) Smith, G.; Cloutt, B. A.; Lynch, D. E.; Byriel, K. A.; Kennard, C. H. L. *Inorg. Chem.* **1998**, *37*, 3236–3242. (b) Xu, A.-W.; Su, C.-Y.; Zhang, Z.-F.; Cai, Y.-P.; Chen, C.-L. *New J. Chem.* **2001**, *25*, 479–482. (c) Wang, Y.-H.; Chu, K.-L.; Chen, H.-C.; Yeh, C.-W.; Chan, Z.-K.; Suen, M.-C.; Chen, J.-D.; Wang, J.-C. *CrystEngComm* **2006**, *8*, 84–93. (d) Lin, C.-Y.; Chan, Z.-K.; Yeh, C.-W.; Wu, C.-J.; Chen, J.-D.; Wang, J.-C. *CrystEngComm* **2006**, *8*, 841–846. (e) Luo, G.-G.; Huang, R.-B.; Chen, J.-H.; Lin, L.-R.; Zheng, L.-S. *Polyhedron* **2008**, *27*, 2791–2798. (f) Luo, G.-G.; Huang, R.-B.; Zhang, N.; Lin, L.-R.; Zheng, L.-S. *Polyhedron* **2008**, *27*, 3231–3238. (g) Yang, H.-L.; Yang, S.; Qiu, X.-Y.; Shao, S.-C.; Ma, J.-L.; Sun, L.; Zhu, H.-L. *Z. Kristallogr.* **2004**, *219*, 157–158. (h) Chi, Y.-N.; Huang, K.-L.; Cui, F.-Y.; Xu, Y.-Q.; Hu, C.-W. *Inorg. Chem.* **2006**, *45*, 10605–10612. (i) Zhu, H.-L.; Yang, S.; Ma, J.-L.; Qiu, X.-Y.; Sun, L.; Shao, S.-C. *Acta Crystallogr., Sect. E* **2003**, *59*, 1046–1047. (j) You, Z.-L.; Zhu, H.-L. *Acta Crystallogr., Sect. C* **2004**, *60*, 623–624. (k) Luo, G.-G.; Sun, D.; Xu, Q.-J.; Zhang, N.; Huang, R.-B.; Lin, L.-R.; Zheng, L.-S. *Inorg. Chem. Commun.* **2009**, *12*, 436–439.
(18) Lotte, K.; Plessow, R.; Brockhinke, A. *Photochem. Photobiol. Sci.* **2004**, *3*, 348–359.
(19) Plessow, R.; Brockhinke, A.; Eimer, W.; Kohse-Höinghaus, K. *J.Phys. Chem. B* **2000**, *104*, 3695–3704.
(20) Sheldrick, G. M. *SHELX-97, program for crystal structure refinement*; University of Göttingen: Göttingen, Germany, 1997.

(t, J(F,F) = 22.4 Hz, 1F), −162.7 (dt, J(F,F) = 24.0 Hz, J(F,F) = 6.9 Hz 2F) ppm. ^{13}C NMR (125 MHz, $(CD_3)_2SO$): δ = 163.4, 158.6, 143.7 (m), 140.5 (m) 137.3 (m), 111.1 (dt, J(C,F) = 18.3 Hz, J(C,F) = 2.3 H), 108.5 ppm. IR (ATR): $\tilde{\nu}$ = 3157, 1693, 1610, 1519, 1487, 1377, 984, 950, 848, 799 cm^{-1}. HRMS (ESI): m/z calcd for $C_{10}H_5F_5N_3$+H$^+$ [M+H]$^+$: 262.03981; found 262.03982. DSC: 523 K (250 °C) melting under decomposition. Anal. found: C 46.28, H 1.57, N 16.09; $C_{10}H_4F_5N_3$ requires C 45.99, H 1.54, N 16.09.

Details of Crystallization. The 2-aminopyrimidine **2** was solved in a hot alcohol (ethanol, in the case of **5** 2-propanol) under sonication to give a saturated solution. Then a concentrated solution of the silver(I) salt in the used alcohol was added. Crystals of macroscopic size precipitated by slow evaporation (hours to days) at room temperature.

$[Ag(\mathbf{2})(CO_2CF_3)]_n$ (**3**). IR (ATR): $\tilde{\nu}$ = 3308, 3179, 1638, 1611, 1491, 1430, 1378, 1184, 1141, 1109, 1090, 986, 944, 838, 795, 723, 490 cm^{-1}. DSC: 484 K (211 °C) melting. Anal. found: C 30.17, H 0.66, N 8.72; $C_{12}H_4AgF_8N_3O_2$ requires C 29.90, H 0.84, N 8.72.

$[Ag(\mathbf{2})(SO_3CF_3)\cdot EtOH]_n$ (**4**). IR (ATR): $\tilde{\nu}$ = 3410, 3330, 3232, 1644, 1610, 1492, 1378, 1246, 1223, 1166, 1026, 987, 961, 635, 510, 489 cm^{-1}. DSC: 381 K (108 °C) ethanol extrusion, 529 K (256 °C) melting and decomposition of the residual compound, which is indicated by a second cooling and heating cycle. Anal. found: C 28.12, H 1.73, N 7.49; $C_{13}H_{10}AgF_8N_3O_4S$ requires C 27.68, H 1.79, N 7.45.

$[Ag(\mathbf{2})(SO_3CF_3)\cdot {}^iPrOH]_n$ (**5**). IR (ATR): $\tilde{\nu}$ = 3419, 3332, 3233, 1650, 1610, 1496, 1377, 1221, 1204, 1169, 1018, 986 cm^{-1}. DSC: 378 K (105 °C) 2-propanol extrusion, 529 K (273 °C) melting and decomposition of the residual compound, which is indicated by a second cooling and heating cycle. Anal. Found: C 28.98, H 2.04, N 7.45; $C_{14}H_{12}AgF_8N_3O_4S$ requires C 29.08; H 2.09, N 7.27.

$[Ag(\mathbf{2})(NO_3)]_n$ (**6**). IR (ATR): $\tilde{\nu}$ = 3321, 3219, 1636, 1498, 1375, 1148, 1071, 1037, 987, 850 cm^{-1}. DSC: 501 K (228 °C) decomposition. Anal. Found: C 27.31, H 0.84, N 12.92; $C_{10}H_4AgF_8N_4O_3$ requires C 27.87, H 0.94, N 13.00.

$[Ag(\mathbf{2})(SO_3CF_3)]_n$ (**7**). Compound **7** was obtained by heating **4** for 15 min to 120 °C quantitatively respectively by heating **5** for 40 min to 120 °C quantitatively.

Obtained from **4**: IR (ATR): $\tilde{\nu}$ = 3330, 3229, 1650, 1610, 1493, 1375, 1281, 1206, 1090, 1017, 986, 944, 852, 794, 633, 514, 483 cm^{-1}. DSC: 529 K (273 °C) melting and decomposition, which is indicated by a second cooling and heating cycle. Anal. Found: C 24.97, H 0.69, N 8.13; $C_{11}H_4AgF_8N_3O_3S$ requires C, 25.50, H, 0.78, N, 8.11. Obtained from **5**: IR (ATR): $\tilde{\nu}$ = 3330, 3229, 1650, 1610, 1493, 1375, 1281, 1206, 1090, 1017, 986, 944, 852, 794, 633, 514, 483 cm^{-1}. DSC: 529 K (273 °C) melting and decomposition, which is indicated by a second cooling and heating cycle. Anal. Found: C 24.37, H 0.62, N 7.99; $C_{11}H_4AgF_8N_3O_3S$ requires C 25.50; H 0.78, N 8.11.

CCDC 749826−749829 contains the supplementary crystallographic data for this paper. These data can be obtained free of charge from The Cambridge Crystallographic Data Centre via www.ccdc.cam.ac.uk/data_request/cif.

Results and Discussion

The pentafluorophenyl functionalized 2-aminopyrimidine **2** was synthesized starting from the aromatic acetic acid derivative to give the iminium salt **1**. In the next step the iminium salt was transformed into the 2-aminopyrimidine **2** by reaction with guanidine hydrochloride (Scheme 1).[21,22]

Scheme 1. Synthesis of the Pentaflourophenyl 2-Aminopyrimidine 2[a]

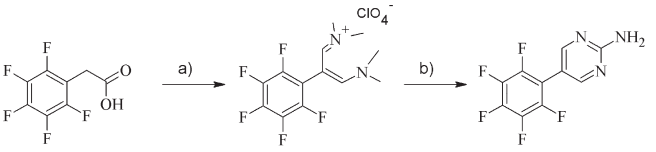

1 2

[a] (a) (i) $POCl_3$, DMF, (ii) $Mg(ClO_4)_2$, 83%; (b) ^{t}BuOH, NaO^{t}Bu, guanidine hydrochloride, 83%.

The silver coordination polymers $[Ag(2)X]_n$ (X = $CO_2CF_3^-$; $SO_3CF_3^-$; NO_3^-) (**3**−**6**, Figure 1) were grown from a saturated alcoholic solution to yield single crystals. For the compounds (**3**−**6**) the single crystal X-ray analyses reveal one-dimensional strands of alternating silver-aminopyrimidine coordination polymers. The asymmetric unit consists of one silver atom, the counterion, and one molecule of **2**. In the case of **4** and **5** also one solvent molecule is included in the asymmetric unit (removed for clarity in Figure 1). The polymer strands of the compounds **3**−**6** differ in selected interatomic parameters like the dihedral torsion angle of the two arene moieties (which is responsible for the delocalization of the π-systems) and the distance and the angle of the silver−nitrogen contacts.

Parameters taken from the single crystal analyses are summarized in Table 1. For structures **4**−**6** a head-to-head alignment of the heterocyclic moiety of neighboring aminopyrimidines is found, while in compound **3** the aminopyrimidines are aligned parallel to each other.

The crystalline compounds **4** and **5** form frameworks with pores which are filled by alcohol solvent molecules used for crystallization. The alcohol can be reversibly removed thermally to yield compound **7** (see below).

The optical properties of the semiconducting materials were investigated by UV−vis absorption and luminescence spectroscopy. The 2-aminopyrimidine-silver complexes **3**, **4**, and **7** show an exclusive solid state emission in the visible region of light. In solution (tetrahydrofuran, ethanol, trifluoroethanol, acetonitrile, cyclohexane, dichloromethane, chloroform) identical optical spectra when compared to the parent compound **2** are found implying that the coordination polymers are not present in solution. The optical properties of compounds **2**−**7** are summarized in Table 2. The ligand **2** is well soluble in ethanol and shows the typical characteristics of a six π-electron arene (Figure 2): Both, absorption and emission occurs in the UV-region and a Stokes-shift of 10325 cm^{-1} and a quantum yield of 0.012 is found.

The absorption spectrum consists of a superposition of two bands. The stronger absorbance is found at shorter wavelengths (263 nm), and it is significantly more sensitive to the solvent polarity in contrast to the other absorption band (296 nm). The emission spectrum of **2** in solution (ethanol, $c = 1 \times 10^{-4}$ M) displays only one unresolved band. The optical properties of **2** in solution were

(21) Jutz, C.; Kirchlechner, R.; Seidel, H.-J. *Chem. Ber.* **1969**, *102*, 2301–2318.

(22) Arnold, Z. *Collect. Czech. Chem. Commun.* **1961**, *26*, 3051–3058.

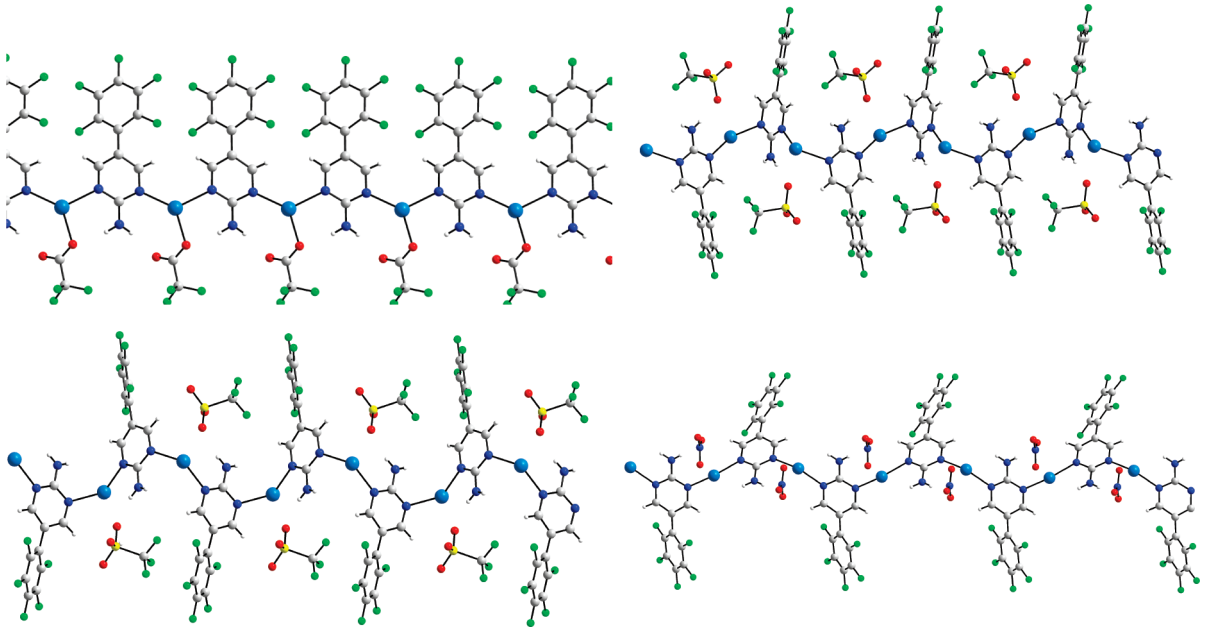

Figure 1. Polymer strand of silver(I) and 2-aminopyrimidine **2**. Top left: compound **3**; bottom left: compound **4**; top right: compound **5**; bottom right: compound **6**.

Table 1. Selected Internuclear Angles and Distances

compound	composition	aryl-aminopyrimidyl dihedral angle [deg]	*d*(N−Ag) [Å]	N−Ag−N angle[Å]	crystal system and space group
3	$[Ag(\mathbf{2})CO_2CF_3]_n$	37.6(2)	2.241(2) 2.301(2)	127.7(1)	triclinic; $P\bar{1}$
4	$[Ag(\mathbf{2})SO_3CF_3\cdot(EtOH)]_n$	41.1(2)	2.276(1) 2.291(1)	126.3(1)	monoclinic; $C2/c$
5	$[Ag(\mathbf{2})SO_3CF_3\cdot(^i PrOH)]_n$	41.7(2)	2.257(2) 2.320(2)	122.1(1)	monoclinic; $P2_1/c$
6	$[Ag(\mathbf{2})NO_3]_n$	44.5(2)	2.241(2) 2.250(2)	156.9(1)	monoclinic; $P2_1/c$

Table 2. Optical and Thermodynamical Parameters[a]

compound	composition	λ_{abs} [nm][b]	λ_{ex} [nm][c]	λ_{em} [nm][c]	optical band gap [eV][e]	$T_m/T_{dec}/T_{se}$[g][°C]
2		263; 296[d]	263; 296[d]	361[d]		
		330	343	387	3.61	250/250/*NA*
3	$[Ag(\mathbf{2})CO_2CF_3]_n$	331; 275	354	502; 390	3.50	211/234−258/*NA*
4	$[Ag(\mathbf{2})SO_3CF_3\cdot(EtOH)]_n$	318; 262	355	481; 377	3.49	*NA*/*NA*/108[h]
5	$[Ag(\mathbf{2})SO_3CF_3\cdot(^i PrOH)]_n$	310; 256	*NA*	375	3.37[f]	*NA*/*NA*/105[h]
6	$[Ag(\mathbf{2})NO_3]_n$	317; 263	*NA*	*NA*	3.46[f]	*NA*/228/*NA*
7[j]	$[Ag(\mathbf{2})SO_3CF_3]_n$	346; 278	358	495; 372	3.46	256[i]/*NA*/*NA*

[a] *NA* = Not available. [b] From glass substrate thin films. [c] In the solid state from single crystals if not indicated otherwise. [d] In ethanol solution ($c = 1 \times 10^{-4}$ M). [e] Calculated from the excitation maximum if not stated otherwise. [f] Calculated from the UV−vis absorption onset. [g] T_m, melting temperature; T_{dec}, temperature of decomposition; T_{se}, temperature of solvent extrusion. [h] First heating cycle to 140 °C. [i] Second heating cycle after solvent extrusion. [j] From polycrystalline sample.

also investigated in various solvents (see above). A plot of the Stokes-shift versus the solvent polarization parameter shows a slight decrease of the shift indicating that the excited state dipole of **2** is smaller than the ground state dipole. In the solid state the absorption and emission spectrum of **2** is significantly red-shifted ($\Delta\nu_{abs} = 7710\ cm^{-1}$; $\Delta\nu_{em} = 1910\ cm^{-1}$) (Figure 2).

The difference in energy of the maximum of absorption in solution and in the solid state corresponds to 0.96 eV (0.23 eV for the emission). This energy shift represents a high intramolecular interaction in the solid state. Unfortunately, crystals of **2** suitable for single crystal analysis could not be obtained so far. Powder diffraction patterns were recorded from polycrystalline samples precipitated from ethanol and from chloroform. Both powder diffraction patterns are identical, indicating that the intermolecular assembly is not affected by the polarity of a protic and an aprotic solvent. The absorption is in the UV-region and the crystals remain colorless. Interestingly, the solid state excitation spectrum is not congruent with the absorption spectrum. This indicates that different states contribute to the absorption of the crystals of **2**, some are not luminescent and do not decay to luminescent states.

The absorption of the silver(I)-aminopyrimidine coordination polymers **3**−**7** are also significantly shifted toward longer wavelength in contrast to the absorption

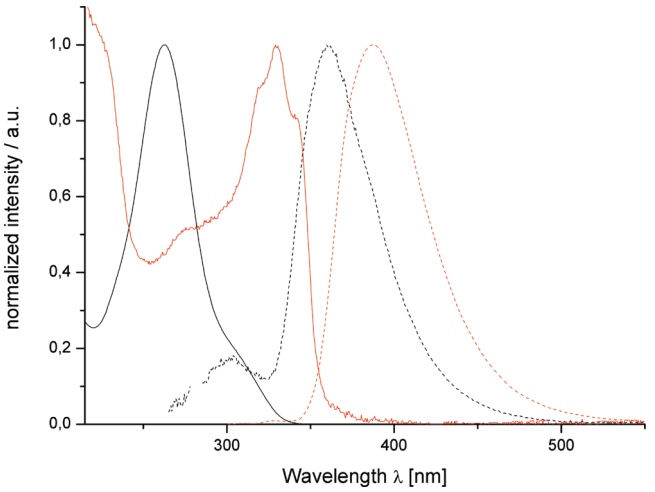

Figure 2. Absorption and emission spectra of the pentaflouro-2-amino-pyrimidine **2** in solution (black) and solid state (red).

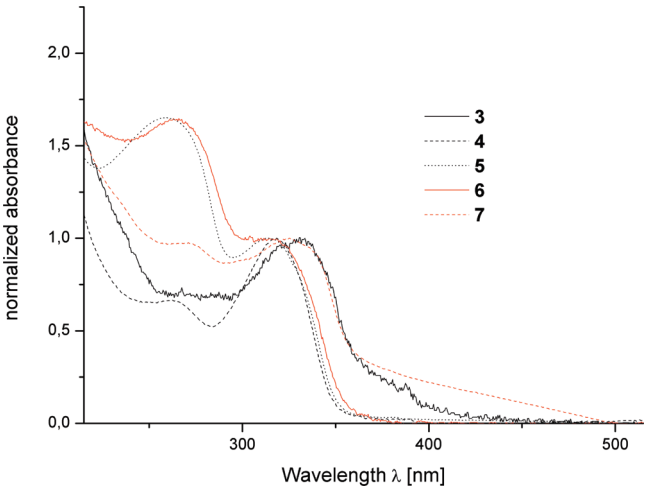

Figure 3. Solid state absorption spectra of the coordination polymers **3**−**7**.

in solution of the parent compound **2** (Figure 3) because of a high degree of intramolecular interaction in the solid state.

For all compounds (**3**−**7**) two absorption maxima are found. One maximum at shorter wavelength in the region of the compound **2** in solution and one longer wavelength absorption which is due to an electronic delocalization of the self-assembled polymers in the solid state. No significant intermolecular interaction for compounds **4**−**6** of neighboring polymer strands in the crystal lattice is found. For compound **3** an offset π-stacking interaction of the perflourinated arenes of neighboring polymer strands can be found. The centroid distance is 3.71 A which implies only a weak interaction.[23] Since an electronic interaction is found in the absorption spectra for all compounds we assume the delocalization takes place within the polymer strands and electronic interstrand interactions are inferior.

Additionally, compounds **3**, **4**, and **7** show an exclusive solid state emission in the visible region. The optical spectra are shown in Figure 4.

A weak emission is found in the wavelength region of the solid parent compound **2**, but it is not identical. For **3**, **4**, and **7** a second strong emission band is found in the visible (see TOC photography). The ratio of the different emissions depends on the excitation wavelength which proves that both are independent states. Interestingly, the polycrystalline samples of **4** and **5** (obtained by grinding or heating and soaking in alcohol) do not show a long wavelength emission although the absorption spectra of the single crystalline and the polycrystalline compounds are identical. This indicates that the crystallite size or intrinsic crystal defects are crucial for the emission in the visible region. The luminescent states are usually found at the red edge of the absorption spectrum. After thermal removing of the alcohol in compounds **4** and **5** (to yield compound **7**), the luminescence of **7** shows a marked red shift in contrast to **4** and an additional emission at long wavelengths in contrast to compound **5**. Compound **7** was exclusively obtained as a polycrystalline sample. Therefore, the origin of the luminous states of **7** and **4** might be of a different nature.

The triflates **4** and **5** show an additional interesting solid state feature.

As mentioned above, the solid state structures of **3**−**6** are made of one-dimensional strands of alternating silver and 2-aminopyrimidine units. These strands form a three-dimensional lattice. The crystal lattices of **4** and **5** are porous frameworks. After precipitation the pores are filled with the alcohol used for crystallization (i.e., ethanol, 2-propanol) as shown in Figure 5. In the plane of projection (crystallographic *c*-axis) two polymer strands are arranged as mirror images to each other; therefore the silver atoms misleadingly seem to be coordinated by four aminopyrimidines in this figure (for clearance see Figure 1). The coordination polymers are aligned vertically, and the interatomic parameters of **4** and **5** are similar (see Table 1). The main difference between the structures of **4** and **5** is that single strands of **4** are aligned parallel to each other but are displaced by a half repetition unit along the *b*-axis whereas single strands of **5** are aligned without structural displacement along the *b*-axis. The incorporated alcohol can be removed by heating and causes a reversible phase transition, since addition of the alcohol regenerates the primary phase. Furthermore, compounds **4** and **5** can be reversibly converted into each other by heating and subsequent addition of the other solvent. In Figure 6 are shown the powder diffraction patterns of the reversible phase transitions of a polycrystalline sample of **4** into **5** via **7**.

By elemental analysis the composition of **4** after heating was determined as $[Ag(\mathbf{2})SO_3CF_3]$ (**7**). Also, heating of **5** causes a phase transition under solvent extrusion yielding **7**. Heating **4** yields the unsolvated compound **7**, which has both lattice parameters and optical properties that are significantly different from those of **4** (Table 2). As mentioned above, the disappearance of the long wavelength emission of polycrystalline **4** possibly correlates to the crystallite size. But this is no explanation for the very large difference of the optical properties of single crystalline **4** and **5** in contrast to the much similar solid state

(23) Janiak, C. *J. Chem. Soc., Dalton Trans.* **2000**, 3885–3896.

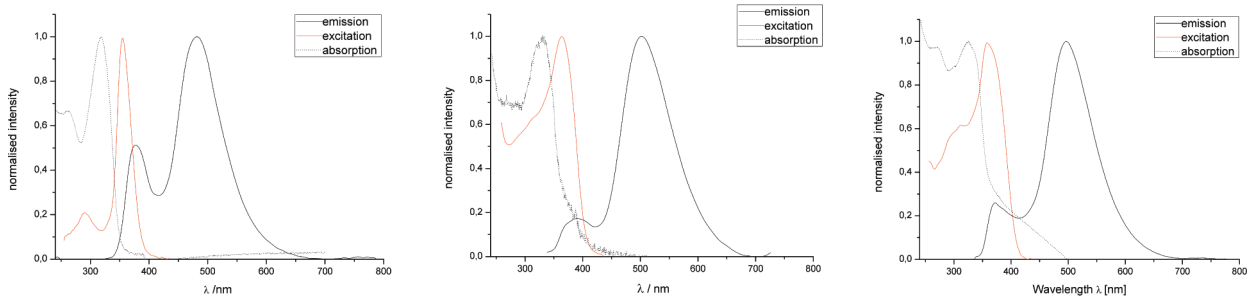

Figure 4. Solid state absorption, emission, and excitation spectra of the coordination polymers **3**, **4**, and **7**.

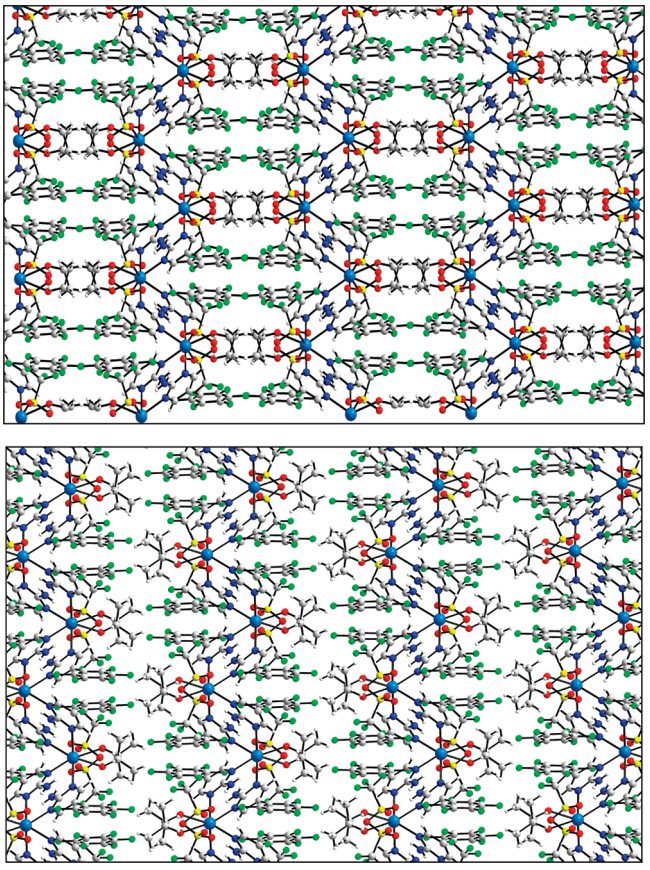

Figure 5. Porous frameworks of **4** (top) and **5** (bottom). View along the crystallographic *c*-axis. The polymer strands precede vertically (along the crystallographic *b*-axis).

structures since single crystals of **5** are also non luminous. We can clearly exclude impurity effects since we have reproduced **4** and **5** many times from many different batches of the starting material and different batches of the silver salts (also different manufacturers) and solvents. Presently, a detailed theoretical investigation of the band structure of the polymer compounds is under progress to give deeper insights into the origin of the luminous states.

Also, **7** can be soaked in water causing a conversion. Herein, 1 equiv of the silver triflate is dissolved in water and removal of the aqueous solution yields a polycrystalline 2:1 complex of **2** and silver triflate and 1 equiv of water. The composition of this compound is confirmed by elemental analysis and an ^{19}F-NMR experiment (for the

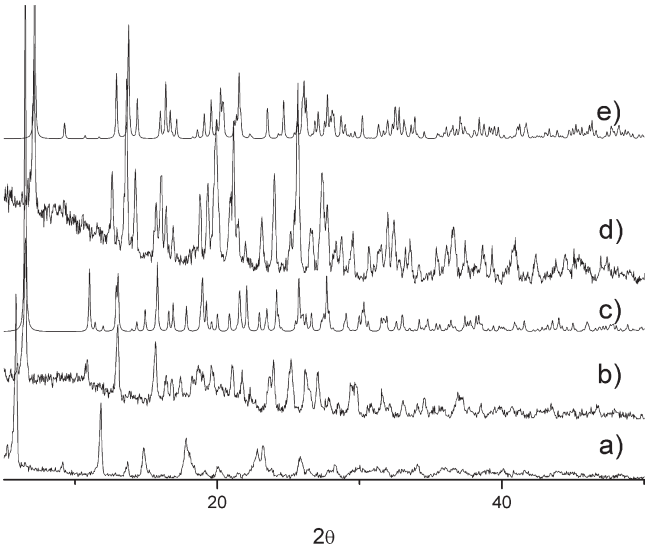

Figure 6. Powder diffraction patterns of the reversible phase transitions of **4** and **5** starting from compound **4**. (a) **4** after heating, 15 min, 120 °C to yield **7**; (b) sequential addition of ^{i}PrOH; (c) Calculated from the single crystal analysis of **5** (100 K); (d) After heating, 40 min, 120 °C and sequential addition of EtOH; (e) Calculated from the single crystal analysis of **4** (100 K). The calculated spectra are slightly shifted to larger θ values due the different measurement temperatures.

XRPD pattern see Supporting Information Figure S3).[24] The water included in the crystal lattice is indicated by the IR resonance at 3439 cm^{-1}. This resonance is exclusively found for compounds with a solvent molecule in the crystal lattice. These solvent induced phase transitions can be achieved by thermal solvent extrusion and sequential solvent addition as well as by chemical equilibration. Furthermore, crystals of **4** can be stored in water or 2-propanol without previous heating, and a phase transition occurs by reaching the chemical equilibrium (water: immediately; 2-propanol: overnight). To evaluate phase transitions, compounds **2**−**7** were investigated by differential scanning calorimetry (DSC, see Table 2). The parent compound **2** melts under decomposition at 250 °C. The nucleation temperature is influenced by the amount of decomposed **2** present upon cooling. Compound **3** melts at

(24) The polycrystalline compound was dissolved in ethanol, and a ^{19}F-NMR was recorded. The ratio of the resonances of the silver salts and **2** matches a 2:1 complex composition (2 equiv of **2** and 1 equiv of $AgSO_3CF_3$). IR (ATR): $\tilde{\nu}$ = 3439, 3347, 3242, 1650, 1608, 1490, 1393, 1279, 1188, 1168, 1016, 984, 850, 628, 586, 482 cm^{-1}. Anal. Found: C 31.62, H 0.96, N 10.60; $C_{21}H_{10}AgF_{13}N_6O_4S$ requires C 31.64; H 1.26, N 10.54.

211 °C and decomposes in two steps at 234 and 258 °C. Compound **6** decomposes without melting at 228 °C. For the triflate compounds **4** and **5** a phase transition under solvent extrusion is found at 108 °C for ethanol and 105 °C for 2-propanol (at a heating rate of 10 K per minute). **7** melts at 256 °C, does not decompose below 300 °C, and does not recrystallize upon cooling.

The conductance of the new material was investigated in a preliminary experiment. From a saturated ethanol solution of compound **4** a thin crystalline film was deposited by drop-casting on a glass substrate. The sample was contacted in a two point probe array with gold contacts and a bias was applied. The conductance under UV-irradiation (385 nm) is not significantly altered in contrast to the conductance under a light bulb. Only a slightly increased conductance is found.[25] The I−V characteristics curves are shown in the Supporting Information (Figure S6).

(25) Because of the anisotropy of the conducting material, a four probe measurement was not applied. The I-V characteristics curve in the darkness is unchanged in reference to the bulb lighted sample. Therefore, since the conducting properties are strongly determined by the Schottky-contact resistance at the semiconductor-metal interface, we also do not derive any physical data from these experiments at this point, and we do not discuss a participation of the photo excited state in the charge transport mechanism based on these preliminary experiments. The characterization of the electrical conductivity requires more experimental and theoretical work, and therefore this preliminary conductivity experiment proves only the general conductance and the applicability for device fabrication of the material.

Conclusion

A new class of silver(I)-organic hybrid semiconducting materials is found suitable for optoelectronic devices. By single crystal X-ray analysis it is found that crystal lattices are made of 1-dimensional polymer strands. The optical band gap and the emissive state can be adjusted by the counterion, the solvent used for crystallization, as well as by reversible solid-state phase transitions of the porous compounds **4** and **5**. Herein, the optical properties of **4** are strongly influenced by the size of the crystallites.

Acknowledgment. This work was supported by the Deutsche Forschungsgemeinschaft (DFG). The authors are also grateful to Hartmut Bögge, Anja Stammler, Markus Meinert, and Partick Thomas for the effort in powder diffraction, to Naoufal Bahlawane for effort in conductivity measurements.

Supporting Information Available: Spectra of optical measurements, powder diffraction patterns, crystal data, and packing diagrams. This material is available free of charge via the Internet at http://pubs.acs.org.